On the formation of carbonic acid (H$_2$CO$_3$) in solar system ices

Weijun Zheng [a,b], Ralf I. Kaiser [b,*]

[a] *Institute for Astronomy, University of Hawaii, Honolulu, HI 96822, United States*
[b] *Department of Chemistry, University of Hawaii, Honolulu, HI 96822, United States*

Abstract

We investigated the irradiation of H$_2$O–CO$_2$ ice mixtures with energetic electrons in an ultrahigh vacuum chamber. Our laboratory studies confirm that – besides carbon monoxide–carbonic acid (H$_2$CO$_3$) is the dominant reaction product of these irradiation processes. We present the kinetics and dynamics of its formation and elucidate on the temperature-dependence (10–60 K) of the formation processes. Our experimental results indicate that carbonic acid might be present in the solar system ices that contain both water (H$_2$O) and carbon dioxide (CO$_2$) and are exposed by radiation from the solar wind and planetary magnetospheres.
Published by Elsevier B.V.

1. Introduction

Unraveling the synthetic routes to form carbonic acid (H$_2$CO$_3$) is of great interest to astrochemists and astrobiologists [1,2]. This acid is a potential reactant to form biologically important molecules like oxalic acid and also has geochemical implications such as the precipitation of carbonates in aqueous solutions [3]. Water and carbon dioxide are the most likely sources of interstellar H$_2$CO$_3$ based on their high cometary [4] and interstellar abundances [5]. Also, both precursors have been found on the surfaces of Europa, Ganymede [6], and Mars [7]. These surfaces are exposed to high energy particles (solar wind, planetary magnetospheres) which can induce a chemical alteration of the pristine environment via non-equilibrium chemistry [8]. Therefore, ices containing water and carbon dioxide are expected to be a residence for carbonic acid. Satellites of Jupiter (Europa, Ganymede and Callisto) are showered with magnetospheric ions [9]. These species can interact with ices and create cascades of secondary electrons in the track of the implanted ions. Due to the absence of a magnetic field, Mars is not bombarded by magnetospheric

ions, but its relative proximity to the sun and lack of dense atmosphere exposes its surface to the solar wind.

Moore and Khanna [10] were the first to study binary mixtures of carbon dioxide and water of a ratio of unity. They discovered carbonic acid after irradiating these ices using 0.7 MeV protons. Dellorusso et al. [11] confirmed this finding; these authors also suggested the formation of formaldehyde (H$_2$CO). Subsequent studies of Brucato et al. [12], Gerakines et al. [13], and Wu et al. [14] demonstrated that formaldehyde is not synthesized in such ices. However, previous studies were conducted at ice temperatures between 10 and 20 K; these temperatures do not mimic the majority of solar system ices that harbor these ice mixtures. Would higher temperature systems, such as Triton (38 K) or Europa (>70 K) or Mars (>133 K), still produce carbonic acid? While many studies have been conducted irradiating ices with protons or ultraviolet (UV) photons, little information exists on the effect of high energy electron exposures. Recall that keV electrons are formed in the track of the galactic cosmic ray and solar wind proton implants once they penetrate the ice layers [6]. Therefore, we present studies of water–carbon dioxide ices and irradiate these binary mixtures at 10, 40, and 60 K with energetic (5 keV) electrons. Most important, only a brief speculation of possible mechanisms to form carbonic acid could be found [13]; this falls short because

* Corresponding author.
E-mail address: ralfk@hawaii.edu (R.I. Kaiser).

the postulated reaction intermediates like radicals and/or ions could not be detected in the experiments. Because neither reaction mechanisms nor rate constants have been derived for the formation of carbonic acid, we found it necessary to conduct an experimental study how carbonic acid is formed in water and carbon dioxide rich ices and how the formation rates depend on the temperature.

2. Experimental

The water–carbon dioxide mixtures were condensed on a silver mirror inside a ultrahigh vacuum (UHV) chamber [15]. A rotatable cold head protrudes from the top of the chamber to steady the silver substrate in the center of the vessel. The temperature of the silver mirror is adjustable from 10 to 340 K by a helium refrigeration system. Connected to the main chamber is an oil-free turbomolecular pump backed by a scroll pump, which allows for pressures to be as low as 7.0×10^{-11} Torr. Attached to the chamber is a differentially pumped electron source, which consists of a tungsten filament and electrostatic lenses to accelerate the electrons to 5 keV. The gas mixture was prepared in a separate side chamber connected by a linear transfer mechanism to the main recipient. Twenty mbar of distilled and repeatedly defrosted water was added to 33 mbar of carbon dioxide (BOC Gases, 99.999%) before condensed for 7 min at a pressure of 7.0×10^{-9} Torr onto the 10 K silver wafer. Fig. 1a shows an infrared spectrum of the pristine ice mixture taken at 10 K; the infrared absorptions are compiled in Table 1. Utilizing a modified Lambert–Beer law [15], the column densities were calculated to be $(1.9 \pm 0.1) \times 10^{17}$ molecules cm^{-2} for H$_2$O and $(4.6 \pm 0.1) \times 10^{17}$ molecules cm^{-2} for CO$_2$. This translates to a carbon dioxide–water ratio of about (2.5 ± 0.5):1. Absorption coefficients for H$_2$O at 3663 cm^{-1} (2.0×10^{-16} cm molecule^{-1}) and CO$_2$ at 2341 cm^{-1} (1.0×10^{-16} cm molecule^{-1}) were taken from Ref. [16,17], respectively. Based on the densities – CO$_2$: 1.7 g cm^{-3} [18], H$_2$O: 0.93 g cm^{-3} [19] – the equivalent thicknesses of the H$_2$O and CO$_2$ were found to be 62 and 190 nm, respectively.

All ices were prepared at 10 K, and were warmed up to a specific temperature (10, 40 or 60 K) prior to an irradiation with 5 keV electrons for 3 h at an electron current of 100 nA. Note the electron beam covers an area of 1.86 ± 0.02 cm^{-2}. A Monte Carlo simulation (CASINO) [20] was used to model the electron trajectory in this ice mixture. In this simulation, the absorbed dose was found to be 8.2 ± 0.3 eV per carbon dioxide molecule and 4.6 ± 0.4 eV per water molecule. Considering the average energy flux on the ice surface of Europa of 10^{13} eV cm^{-2} s^{-1} [21] and comparing this value with our simulation conditions, we can estimate that 1 s in our laboratory experiments mimics about 100 s of radiation exposure of Europa's icy surface. A blank experiment was conducted in a similar way as the real experiments, but without exposing the samples to the electron beam. To ensure that all the reaction products were stable, the samples were kept under
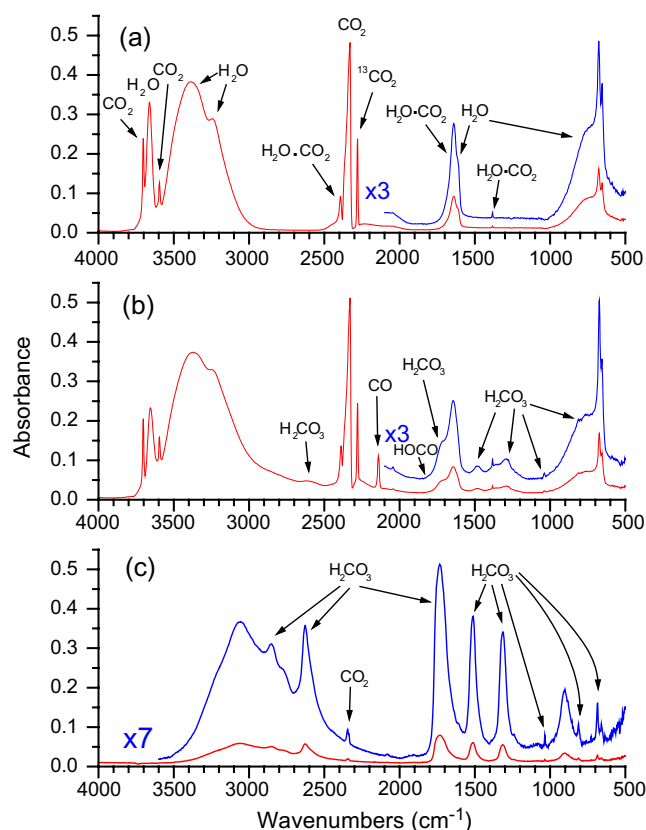

Fig. 1. (a) Infrared spectrum of the unirradiated H$_2$O/CO$_2$ ice at 10 K. (b) H$_2$O/CO$_2$ infrared spectrum at 10 K after 3 h of irradiation with 100 nA electrons. H$_2$CO$_3$ and CO were the major products. A very small CO$_3$ peak was found at 2044 cm^{-1} but not labeled in the figure. (c) Infrared spectrum of the irradiated sample warmed up to 210 K. This spectrum was collected after 3 h of irradiation at 10 K and warmed to 210 K.

Table 1
The infrared absorption frequencies in the infrared spectrum for water and carbon dioxide in an ice mixture at 10 K, compared to experimental frequencies performed with pure H$_2$O and pure CO$_2$

Observed wavenumber (cm^{-1})	Literature wavenumber (cm^{-1})	Molecule	Vibration
4030	3947	H$_2$O · CO$_2$	v_3
3795	3818	H$_2$O · CO$_2$	v_1
3702	3707	CO$_2$	$v_1 + v_3$
3661	3653	H$_2$O	v_1
3595	3602	CO$_2$	$2v_2 + v_3$
3385	3332	H$_2$O	v_3
3240	3151	H$_2$O	v_3
2393	2404	H$_2$O · CO$_2$	v_3
2330	2341	CO$_2$	v_3
2280	2281	CO$_2$	v_3
1638	1626	H$_2$O · CO$_2$	v_2
1614	1574	H$_2$O	v_2
1384	1384	CO$_2$	v_1
750	760	H$_2$O	v_1
677 654	660 654	CO$_2$	v_2 [a]
660 654	663 649	H$_2$O · CO$_2$	v_2 [a]

H$_2$O is the literature values and assignments from Ref. [16,22].
CO$_2$ is the literature values and assignments from Ref. [17].
H$_2$O · CO$_2$ is the literature values and assignments taken from Ref. [23].
[a] In-plane bend, out-of-plane bend.

isothermal conditions for 1 h. For example, the samples irradiated at 40 K or 60 K were isothermally held at those temperatures for one hour, and then cooled to 10 K. Afterward, the ice samples were warmed slowly (0.5 K min^{-1}) from 10 to 280 K. The species in the gas phase were monitored by a Balzer QMG 420 quadrupole mass spectrometer. During the entire experiment, infrared spectra were continuously recorded every 2 min to monitor the chemical modifications of the ice samples.

3. Results

The first step in the analysis of the data is to examine the initial, pre-irradiated infrared spectrum of the carbon dioxide–water mixture. Based on previous experiments of pure H_2O [16], pure CO_2 ices [15,17] and H_2O/CO_2 ice mixtures [22], eleven peaks can be identified as fundamental or combination bands, five belonging to the water and six absorptions to the carbon dioxide (Table 1; Fig. 1a). Ab initio calculations carried out by Danten et al. [23] indicate the remaining peaks belong to a H_2O–CO_2 complex. These absorptions match up well with the peaks found in our experiments, except for the O–H stretch (v_3), which was off by about 85 cm^{-1}. The peaks at 660 and 654 cm^{-1} are hidden under the carbon dioxide absorptions, but become visible at 110 K in the warm-up phase after the carbon dioxide has sublimed.

After the sample was irradiated for 180 min, the spectrum clearly shows the presence of carbonic acid (Fig. 1b); six fundamentals were detected and correlate well with the literature data. A list of the wavenumbers and the assignments can be found in Table 2. Two peaks at 690 and 2850 cm^{-1} are not seen until after the warm-up of the irradiated sample. At 210 K, very little of the water, carbon dioxide, and the water–carbon dioxide complex remained; the carbonic acid spectrum becomes much clearer (Fig. 1c). Among all absorptions identified, only one peak at 1483 cm^{-1} did not overlap with the absorptions from water and carbon dioxide; therefore, this absorption was used to calculate column densities of the newly formed carbonic acid as discussed below. Of the nine frequencies observed by Gerakines et al. [13], only one could not be

Table 2
Observed H_2CO_3 infrared frequencies displayed in H_2O/CO_2 ice after 3 h of electron irradiation

Observed wavenumber (cm^{-1})	Literature wavenumber (cm^{-1})[a]	Vibration
2850	2840	O–H stretch
2620	2626	O–H stretch
1723	1719	C=O stretch
1483	1508	COH a-sym stretch
1292	1307	COH in plane bend
1038	1038	COH sym stretch
812	813	CO_3 out of plane bend
685	690	CO_3 in plane bend

[a] Ref. [11,13].
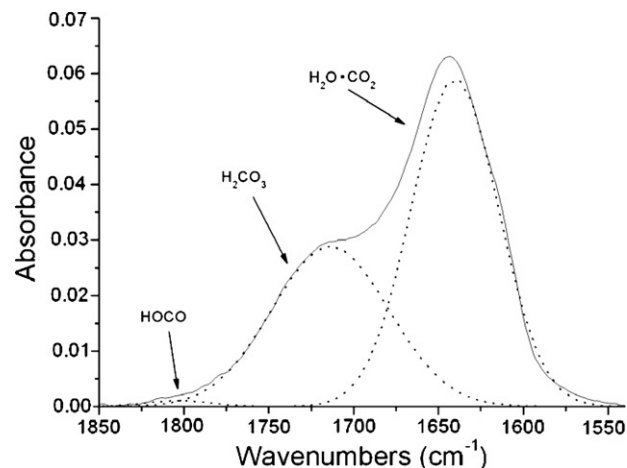

Fig. 2. Deconvoluted peaks of the irradiated infrared spectra (1850–1550 cm^{-1}) at 10 K.

confirmed in our experiments. Even after sufficient heating, the COH out-of-plane bending mode at 908 cm^{-1} could not be witnessed because of lingering water on the silver mirror. Additionally, there is one extra peak to note in the infrared region of irradiated sample (Fig. 1b). The *trans*-HOCO intermediate could be assigned to a peak at 1810 cm^{-1} (Fig. 2). Milligan and Jacox [24] identified *cis* and *trans*-HOCO radicals at 1797 and 1833 cm^{-1} respectively. We suggest that the 1810 cm^{-1} peak is from *trans*-HOCO, at a slightly lower wavenumber, due to the red shifting effect of our H_2O matrix (unlike Milligan's 99% CO matrix).

Besides the absorptions from carbonic acid and *trans*-HOCO, the electron irradiation of the water–carbon dioxide ices only produced two additional products. These are carbon monoxide (CO) and the cyclic carbon trioxide isomer (CO_3). Both molecules were identified via their absorptions at 2140 and 2044 cm^{-1}. These positions agree well with previous band assignments [15,17]. No hydrogen peroxide (HOOH) was seen in the FTIR spectra, but could be assigned to the proper mass to charge ratio, m/z, of 34 as witnessed by the quadrupole mass spectrometer (QMS). In the blank experiment, no ion current was received for $m/z = 34$, but in all three irradiations, a small amount was observed. The peak for this mass-to-charge formed just after the sublimation of water at 190 K, and was approximately three orders of magnitude lower than H_2O. Formaldehyde (H_2CO) and formic acid (HCOOH) were not detected by the FTIR. As noted by Wu et al. [14] in their H_2O/CO_2 experiments, the carbonyl stretch from H_2CO (1720 cm^{-1}) could be hidden underneath the broad peak of carbonic acid, we are not able to confirm the formation of H_2CO. In our QMS data, HCOOH ($m/z = 46$) was not found in any of the four experiments.

Fig. 3 presents the decay of H_2CO_3 absorption features during the post-irradiation warming up in the temperature range 210–256 K. The decay of these absorption features is correlated to the detection of H_2CO_3 ($m/z = 62$) mass signal in the temperature range. These results indicate that
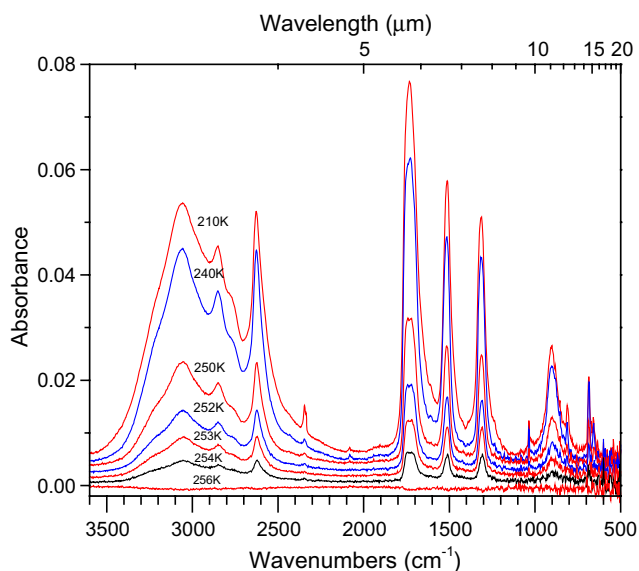
Fig. 3. Decay of the infrared features of the new species upon warming. The H_2O/CO_2 ice was irradiated at 10 K with electrons for 3 h, then, was warmed up to these temperatures. The spectra are offset for clarity.

H_2CO_3 was generated by irradiation and were released into the gas phase at temperature between 210 and 256 K.

4. Discussion

To investigate the evolution of carbonic acid during the irradiation in time, one must understand the kinetics of the reaction. Fig. 4 shows the column density of H_2CO_3 as the ice sample is irradiated. The absorption coefficient (6.5×10^{-17} cm molecule^{-1}) at 1505 cm^{-1} was taken from Gerakines et al. [13]. The best fit includes a two-step mechanism, i.e. $A \rightarrow B \rightarrow C$, where A is the $H_2O \cdot CO_2$ complex, B is an intermediate, and C presents the carbonic acid. To calculate the best fits as shown in Fig. 4, (1)–(3) were used. This leads to the rate constants (Table 3) for the first step from A to B, k_1, and the second step from B to C, k_2. Based on our fits, the changes in rate constants with temperature are not statistically significant. Therefore, at irradiations from 10 to 60 K, neither step is significantly temperature dependent suggesting that non-equilibrium chemistry dictates the chemical processing of the sample. However, the number of $H_2O \cdot CO_2$ complexes formed capable of reacting, $[A]_0$, were found to increase with temperature. This likely indicates that as temperature increases, the number of $H_2O \cdot CO_2$ complexes with the correct orientation geometry for the reaction to form carbonic acid present in the pristine sample increases.

$$[A]_t = [A]_0 e^{-k_1 t} \tag{1}$$

$$[B]_t = [A]_0 \left(\frac{k_1}{k_2 - k_1} \right) (e^{-k_1 t} - e^{-k_2 t}) \tag{2}$$

$$[C]_t = [A]_0 \left[1 - \left(\frac{k_2}{k_2 - k_1} e^{-k_1 t} \right) \left(\frac{k_1}{k_2 - k_1} e^{-k_2 t} \right) \right] \tag{3}$$
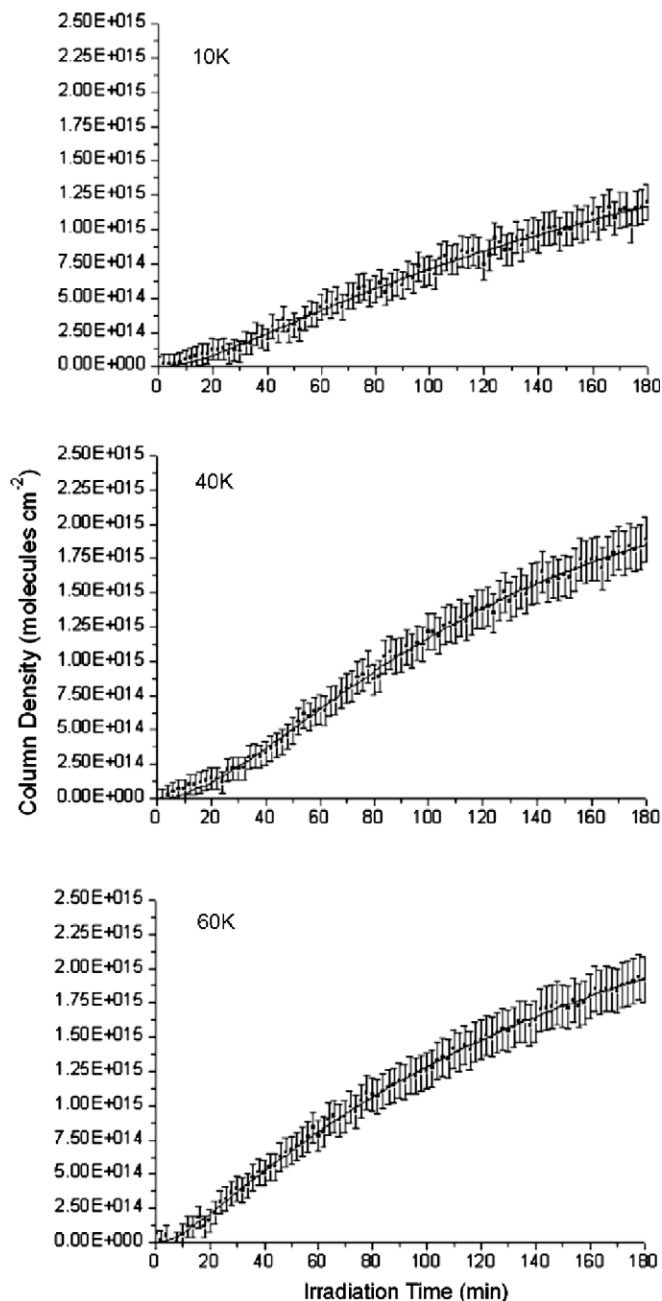

Fig. 4. Temporal evolution of carbonic acid with time at 10 K (top), 40 K (middle), and 60 K (bottom). Experimental data points have been fit via (1)–(3).

Table 3
Rate constants and initial concentration of $H_2O \cdot CO_2$ complexes for a two step mechanism of the temporal evolution of carbonic acid. Numbers based on fits in Fig. 4

T (K)	k_1 (s^{-1})	k_2 (s^{-1})	$[A]_0$ (molecules cm^{-2})
10	$(0.8 \pm 0.4) \times 10^{-4}$	$(1.0 \pm 0.4) \times 10^{-3}$	$(2.1 \pm 0.3) \times 10^{15}$
40	$(1.5 \pm 0.5) \times 10^{-4}$	$(0.6 \pm 0.4) \times 10^{-3}$	$(2.5 \pm 0.2) \times 10^{15}$
60	$(1.1 \pm 0.5) \times 10^{-4}$	$(1.8 \pm 0.6) \times 10^{-3}$	$(2.9 \pm 0.2) \times 10^{15}$

Now that the kinetics has been solved, let us consider the likely reaction mechanism(s). We suggest that the reaction

commences with an electron-induced O–H bond rupture within the water molecule. Once the O–H bond is broken by the electron irradiation, a hydrogen atom (H) and a hydroxyl radical (OH) are formed. Each open shell species has a potential to react with a neighboring CO_2 molecule. Based on these possibilities, we examined two reactions: $H+CO_2$ (4) and $OH+CO_2$ (5). Both reactions are exoergic by the same order of magnitude [25,26]. Conservation of angular momentum and different masses of the hydrogen atom (1 amu) and of the hydroxyl radical (17 amu), the kinetic energy of the hydrogen atom will be significantly greater than that of the hydroxyl radical. The detection of the HOCO radical, but the failed observation of the HOCOO species suggests that the energetic hydrogen atom can add to the carbon dioxide molecule via Eq. (4) even at 10 K:
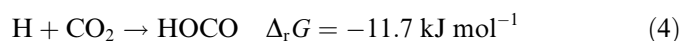
$$H + CO_2 \rightarrow HOCO \quad \Delta_r G = -11.7 \text{ kJ mol}^{-1} \tag{4}$$

$$OH + CO_2 \rightarrow HOCOO \quad \Delta_r G = -26.4 \text{ kJ mol}^{-1} \tag{5}$$

Fig. 5 displays our proposed reaction mechanism. The $H_2O \cdot CO_2$ complex undergoes an electron-induced O–H bond rupture, resulting in a hydrogen atom adding to the carbon–oxygen double bond of the CO_2 molecule. Note that at 10 K, this reaction cannot proceed without irradiation since excess energy is needed to overcome bond ruptures and the total endoergicity of the reaction of 31.4 kJ mol^{-1} to form carbonic acid. Therefore, in the interstellar medium, thermal energy alone will not be sufficient to overcome the large barrier (629.3 kJ mol^{-1}). This potential energy surface requires non-equilibrium chemistry (such as that generated by ionizing radiation). This suprathermal hydrogen now has excess kinetic energy required to overcome the barrier to addition to the carbon

dioxide to form *cis*-HOCO (endoergic by 91.3 kJ mol^{-1}), which has been proposed before by a number of researchers [25,27–29]. It can isomerize (37.6 kJ mol^{-1} barrier) to *trans*-HOCO, and then recombines with the hydroxyl radical to form carbonic acid (exoergic by 471.9 kJ mol^{-1}).

H_2O and CO_2 ices are among the most prevalent ices found in the interstellar medium [5]. They are also known to co-exist on the surface of Mars [7], Triton [30], Jovian satellites [6] and on comets [4]. These ices are exposed to irradiation from comics ray particles, solar wind and/or planetary magnetospheres. Based on our experimental data, carbonic acid would exist in these objects. Mars in particular is of great significance. Without a dense atmosphere, Mars lacks the power to deflect penetrating solar wind, cosmic rays or any type of high energy particles. In the history of Mars, there might be a high concentration of carbonic acid. H_2CO_3 is a water soluble acid and if available in sufficient concentrations, could potentially dissolve metal ores and catalyze chemical reactions. The presence of carbonic acid on Mars may also lead to the existence of limestone ($CaCO_3$), magnesite ($MgCO_3$), dolomite ($CaMg(CO_3)_2$), and siderite ($FeCO_3$) [3]. These chemicals have been tentatively detected on the Martian surface [31].
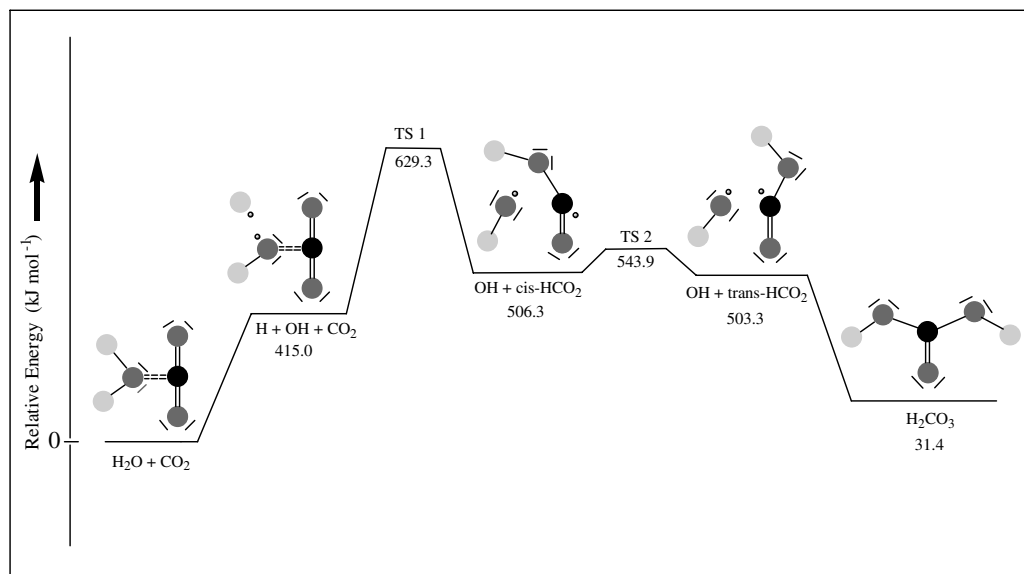
Acknowledgements

Fig. 5. Proposed reaction mechanism for the formation of carbonic acid from water and carbon dioxide. All energetics are relative to $H_2O + CO_2$. Carbon, oxygen and hydrogen atoms are represented by black, dark grey, and light grey circles, respectively.

References

[1] R. Barbieri, B. Cavalazzi, Space life sciences: search for signatures of life, and space flight environmental effects on the nervous system, 2004, p. 1262.

[2] J. Parnell, A. Mazzini, C. Honghan, Astrobiology 2 (2002) 43.

[3] F. Westall, P. Gobbi, D. Gerneke, G. Mazzotti, Microstructures in the carbonate globules of Martian meteorite ALH 84001: preliminary results of a high resolution SEM study, lunar and planetary institute conference abstracts, 1998, p. 1362.

[4] S.J. Kim, Y.C. Minh, S. Hyung, Y.H. Kim, E.F. van Dishoeck, F.F.S. van der Tak, High resolution opticals and infrared observations of molecules in comets chemistry in the envelopes around massive young stars, from molecular clouds to planetary, 2000, p. 471.

[5] P. Ehrenfreund, W.A. Schutte, Infrared observations of interstellar ices, from molecular clouds to planetary, 2000, p. 135.

[6] N.J. Mason et al., VUV spectroscopy of extraterrestrial ices, Astrochemistry – from laboratory studies to astronomical observations, 2006, p. 128–139.

[7] J. Longhi, J. Geophys. Res.-Planets 111 (2006).

[8] R.I. Kaiser, Chem. Rev. 102 (2002) 1309.

[9] J.F. Cooper, R.E. Johnson, B.H. Mauk, H.B. Garrett, N. Gehrels, Icarus 149 (2001) 133.

[10] M.H. Moore, R.K. Khanna, Spectrochim. Acta 47 (1991) 255.

[11] N. Dellorusso, R.K. Khanna, M.H. Moore, J. Geophys. Res.-Planets 98 (1993) 5505.

[12] J.R. Brucato, M.E. Palumbo, G. Strazzulla, Icarus 125 (1997) 135.

[13] P.A. Gerakines, M.H. Moore, R.L. Hudson, Astron. Astrophys. 357 (2000) 793.

[14] C.Y.R. Wu, D.L. Judge, B.M. Cheng, T.S. Yih, C.S. Lee, W.H. Ip, J. Geophys. Res.-Planets 108 (2003).

[15] C.J. Bennett, C. Jamieson, A.M. Mebel, R.I. Kaiser, Phys. Chem. Chem. Phys. 6 (2004) 735.

[16] W. Zheng, D. Jewitt, R.I. Kaiser, Astrophys. J. 639 (2006) 534.

[17] C.S. Jamieson, A.M. Mebel, R.I. Kaiser, Chem. Phys. Chem. 7 (2006) 2508.

[18] J. Klinger, D. Benest, A. Dollfus, R. Smoluchowski, in: Proceedings of the Advanced Research Workshop, Nice, France, January 16–19, 1984, NATO ASIC Proc. 156: Ices in the Solar System, 1985.

[19] P. Jenniskens, D.F. Blake, A. Kouchi, Amorphous water ice. A Solar System Material, ASSL vol. 227: Solar System Ices (1998) 139.

[20] P. Hovington, D. Drouin, R. Gauvin, Scanning 19 (1997) 1.

[21] R.W. Carlson et al., Science 283 (1999) 2062.

[22] K.I. Oberg, H.J. Fraser, A.C. Adwin Boogert, S.E. Bisschop, G.W. Fuchs, E.F. van Dishoeck, H. Linnartz, Astron. Astrophys. 464 (2007) 1187.

[23] Y. Danten, T. Tassaing, M. Besnard, J. Phys. Chem. A 109 (2005) 3250.

[24] D.E. Milligan, M.E. Jacox, J. Chem. Phys. 54 (1971) 927.

[25] K. Kudla, G.C. Schatz, J. Phys. Chem. 95 (1991) 8267.

[26] T.L. Allen, W.H. Fink, D.H. Volman, J. Phys. Chem. 100 (1996) 5299.

[27] X. Song, J. Li, H. Hou, B. Wang, J. Chem. Phys. 125 (2006) 094301.

[28] M.J. Lakin, D. Troya, G.C. Schatz, L.B. Harding, J. Chem. Phys. 119 (2003) 5848.

[29] S.I. Ionov, G.A. Brucker, C. Jaques, L. Valachovic, C. Wittig, J. Chem. Phys. 99 (1993) 6553.

[30] W.M. Grundy, L.A. Young, Icarus 172 (2004) 455.

[31] M. Cabane et al., Mercury, mars and saturn (2004) 2240–2245.